



Numerical Simulation Model Construction of Swept Frequency Dielectric Logging Response Based on Wireless Communication

Liang Pang^(✉)

Public Basic Course Department, Wuhan Institute of Design and Sciences, Wuhan 430025, China
pangliang0611@163.com

Abstract. The current method is faced with the interference of logging signals caused by mud invasion, which cannot meet the real-time requirements. In order to effectively solve geological problems and improve the ability to solve complex formations, it is necessary to carry out numerical simulation of swept frequency dielectric logging response. Therefore, a numerical simulation model of swept frequency dielectric logging response based on wireless communication is proposed. By defining directional signals, the inclined transmitter coil structure has the ability of formation evaluation and geosteering azimuth detection, and a variety of formation models are used for numerical simulation of logging tools. The experimental results show that the numerical simulation model is effective.

Keywords: Wireless Communication · Sweep Frequency Dielectric Logging · Response Value · Simulation Model · Directional Signal

1 Introduction

With the continuous progress of communication technology, wireless communication technology has been widely used in the field of logging. With the rapid development of social economy, the demand for oil resources in the market is also gradually increasing. Because oil is a non renewable resource, the storage capacity is decreasing year by year with the continuous increase of market demand, and the oil storage environment to be exploited is becoming more and more difficult to develop. In actual engineering, more stratum information needs to be obtained before oil exploitation, which is conducive to the maximum benefit of oil exploitation [1, 2]. With the development of Shengli Oilfield, Zhongyuan Oilfield and other large oilfields, the oil and gas difficult to exploit in oil and gas reservoirs are gradually replaced by fresh water or sewage injection, and become a water flooded layer with small or complete water production [3, 4]. However, after water flooding treatment of oil and gas reservoirs, the resistivity changes slightly, and it is impossible to distinguish between water flooded layers and oil and gas reservoirs according to the resistivity change. In order to make the oilfield stable and high-yield for a long time, it is necessary to drill adjustment wells in the original developed well pattern. At this time, the effect of using resistivity parameters to distinguish oil, gas

and water layers is not good [5, 6]. It is gradually found that the propagation process of electromagnetic wave, a physical wave, is not only related to the conductivity of the medium. The higher the frequency of electromagnetic wave, the greater the impact on the dielectric constant. Thus, the dielectric logging for detecting the acoustic properties was developed [7]. The oil reserves are described by using the acoustic velocity and amplitude output from the acoustic logging tool. At the initial development stage of the acoustic logging technology, it is necessary to use a combination of various technologies to obtain formation information. The amount of formation parameters and rock information provided is small, and the reliability is low. With the rapid development of computer technology and measurement and control technology, the development of logging instrument technology has made great progress [8, 9].

At present, relevant scholars have made significant contributions to the development of logging technology. The earliest widely used logging method was to reflect formation information through low-frequency to high-frequency electromagnetic waves. Its basic principle is to use electrical methods to measure underground environmental data. When electromagnetic waves pass through underground formation minerals, different electrical parameters are generated. By analyzing the temporal and spatial distribution of electromagnetic waves at the receiving end, Obtain the distribution status of different minerals underground [10]. With the development of the times, the development of integrated circuits has promoted the logging technology to an unprecedented level, including induction logging, lateral logging, logging while drilling and other logging technologies. For different downhole detection purposes, different logging instruments are used in the actual detection process. Most of these detection mechanisms use logging circuits to form transmission currents or induced electromotive forces around the area to be measured downhole. The receiving end of the logging instrument changes the phase and amplitude by receiving the transmission characteristics of electromagnetic waves, and further calculates the resistivity or conductivity of the formation under logging. However, these methods have strong practicality in situations where there is a significant difference in conductivity between underground formations, and poor practicality in situations where there is a small difference in conductivity between local layers. Therefore, it is necessary to study the response characteristics of downhole resistivity logging directionally to provide Effective theory basis for the realization of oil and gas reservoir evaluation.

To address the above issues, the article proposes a simulation model for the numerical response of swept frequency dielectric logging based on wireless communication. Propose a combination of horizontal and vertical coils to construct inclined coils to detect underground formations, analyze the equivalence between the isotropic protective layer of electrical parameters and its macroscopic anisotropy, and finally comprehensively simulate and evaluate the swept frequency dielectric logging response of multi-layer inclined anisotropic formations. The experimental results show that this model is suitable for analyzing the response of sweep frequency dielectric logging tools with coils placed in any direction. It has the advantages of fast calculation speed and high accuracy, meets real-time requirements, and improves the ability to solve complex formations.

2 Sweep Frequency Dielectric Logging Model and Wireless Communication Method

This study first achieved the measurement of the dielectric constant of underground media by constructing a swept frequency dielectric logging model. In terms of constructing the swept frequency dielectric logging model, the complexity and nonlinear characteristics of the formation were considered, and an accurate and reliable dielectric logging model was established. An optimized inversion method is proposed for wireless communication problems in swept frequency dielectric logging. By optimizing the design of wireless communication between sensor nodes, the reliability and efficiency of data transmission are maximized. This method combines multi-objective optimization algorithms and signal processing techniques to achieve accurate inversion of the dielectric constant of underground media.

2.1 Construction of Swept Frequency Dielectric Logging Model

The swept frequency dielectric logging needs to measure the range of conductivity, measurement resolution and detection depth to select the operating frequency [11–13]. The general swept frequency dielectric logging model is a three coil system structure r_c is the coil radius of swept frequency dielectric logging model, r_w represents the wellbore radius, T represents the transmitting coil, R_1, R_2 represent the near receiving coil and far receiving coil of swept frequency dielectric logging model, $\varepsilon(\vec{r}), \sigma(\vec{r}), \mu(\vec{r})$ representative \vec{r} for the dielectric constant, conductivity and permeability at the location [14, 15], after selecting the downhole background medium, divide and calculate the medium objects with different dielectric and electrical parameters from the downhole background medium, and select the formation with the same properties as the borehole parameters as the background medium, $\varepsilon_0, \sigma_0, \mu_0$ respectively represents the dielectric constant, conductivity and permeability of the downhole background medium [16, 17]. Utilize the amplitude ratio of two receiving coils A_{R1}, A_{R2} and phase difference θ_{R1}, θ_{R2} formation with known sweep frequency dielectric logging conductivity is calibrated, and the amplitude ratio and phase difference are converted into corresponding conductivity, which is expressed by the following formula:

$$\begin{cases} A_R = A_{R1}/A_{R2} \\ P_D = \theta_{R1} - \theta_{R2} \end{cases} \quad (1)$$

Symmetrical compensation coil system is used to describe the boundary between formation and water layer during sweep frequency dielectric logging, measure the conductivity of underground formation at multiple depths, and calculate the voltage on any receiving coil of conductivity by calculating the electronic field generated by magnetic dipole [18, 19]. The finite element method is usually used to integrate the electric field on the coil, which can be obtained by using the magnetic field component in the normal direction of the coil H_{RH} Obtain the finite element wireless communication equation:

$$V_R = j_w \times \mu_0 \times S_R \times H_{RH} \times (A_R + P_D) \quad (2)$$

Where, j_w represents the electromagnetic conductivity of sweep frequency dielectric logging, S_R represents the area of receiving coil of swept frequency dielectric logging conductivity sensor.

Assumptions, ϵ_0 represents the relative permittivity of the swept frequency dielectric measurement of the anisotropic formation background medium, σ_0 represents the conductivity of swept frequency dielectric logging sensor, j represents the current parameter, and uses the following formula to give the Complex permittivity $\hat{\epsilon}_0 = \epsilon_0 - j\sigma_0/\omega$ induced current of swept frequency dielectric logging sensor is defined according to the volume equivalent mechanism $\vec{J}(\vec{r})$ since all induced currents are in uniform downhole formation background medium, the total field of sweep frequency dielectric logging sensor is located in all downhole formation areas $\vec{E}(\vec{r})$ I.e. incident field $\vec{E}^i(\vec{r})$ secondary induction field generated by scattering with downhole formation $\vec{E}^s(\vec{r})$ sum is expressed by the following formula:

$$\vec{E}(\vec{r}) = [\vec{E}^s(\vec{r}) + \vec{E}^i(\vec{r})] \times V_R \tag{3}$$

Where, the scattering field of regular and uniform formation $\vec{E}^s(\vec{r})$ and vector bit $\vec{A}(\vec{r})$ and scalar bit $\phi(\vec{r})$ relevant, $\vec{E}^s(\vec{r}) = -j_w \vec{A}(\vec{r}) - \Delta \phi(\vec{r})$, according to Green's function, downhole formation vector potential $A(\vec{r})$ and swept frequency dielectric logging induced current $\vec{J}(\vec{r}')$ relevant:

$$\vec{A}(\vec{r}) = \frac{\mu_0}{4\pi} \int_V \vec{J}(\vec{r}') \frac{e^{\sigma|\vec{r}-\vec{r}'|}}{|\vec{r}-\vec{r}'|} dv' \times \vec{E}(\vec{r}) \tag{4}$$

Where, \vec{r}' represent the direction of observation point P vector of point, \vec{r} Represents the origin point P Vector of points, scalar bit $\phi(\vec{r})$ related to the volume charge of swept frequency dielectric logging receiving coil:

$$\phi(\vec{r}) = \frac{1}{4\pi\hat{\epsilon}_0} \int_V \rho(\vec{r}') \frac{e^{\sigma|\vec{r}-\vec{r}'|}}{|\vec{r}-\vec{r}'|} k_0 dv' \times \vec{A}(\vec{r}) \tag{5}$$

Where, k_0 represents that in the process of sweep frequency dielectric logging, dv' Jacobi determinant representing regular transformation, $\rho(\vec{r}')$ represents the induced charge density, the wave number in the background medium, where, $k_0 = \omega\sqrt{\hat{\epsilon}_0\mu_0}$ according to the current continuity equation, use the following formula to describe the relationship between the charge density and the induced current of the swept frequency dielectric logging receiving coil:

$$\nabla \vec{J}(\vec{r}) = -j_w \rho(\vec{r}) \times \phi(\vec{r}) \tag{6}$$

Because of the sweep frequency dielectric logging potential shift vector in the background medium $\vec{D}(\vec{r}')$ satisfy $\vec{D}(\vec{r}') = \vec{\epsilon}(\vec{r})\vec{E}(\vec{r})$. Therefore, swept frequency dielectric logging receiving coil inductor current and electric displacement vector meet the following constraints:

$$\vec{J}_v(\vec{r}) = j_w \vec{\kappa}(\vec{r}) \times \vec{D}(\vec{r}') \times \nabla \vec{J}(\vec{r}) \tag{7}$$

Among them, $\tilde{\kappa}(\vec{r})$ stands for contrast tensor, i.e. $\tilde{\kappa}(\vec{r}) = (\vec{\varepsilon}(\vec{r}) - \vec{I}\hat{\varepsilon}_0) \cdot \vec{\varepsilon}^{-1}(\vec{r})$ expression based on the potential shift vector of swept frequency dielectric logging receiving coil can be obtained:

$$\vec{E}^i(\vec{r}) = \vec{D}(\vec{r}') \times \vec{\varepsilon}^{-1}(\vec{r}) + j_w \vec{A}(\vec{r}) + \nabla \phi(\vec{r}) \times \vec{J}_v(\vec{r}) \tag{8}$$

According to the analysis formula (8), under the condition that the frequency of the induced current of the swept frequency dielectric logging receiving coil is not high $\sigma/w \geq \varepsilon$, indicating that the complex permittivity in homogeneous background media is mainly related to frequency and downhole formation conductivity, and the relative permittivity ε has little effect on the response of sweep frequency dielectric logging [20, 21]. The inhomogeneous formation except the underground formation background medium is divided into tetrahedral grids, and the SWG basis function is used to discretize sweep frequency dielectric logging to receive coil displacement current and potential displacement vector. In each tetrahedron, the contrast tensor $\tilde{\kappa}$ are constants, we can obtain:

$$H_{JJ} = Tr(\tilde{\kappa}^{\pm}) \times \vec{E}^i(\vec{r}) \tag{9}$$

where, $Tr(\tilde{\kappa}^{\pm})$ trace representing the matrix, that is, the sum of diagonal elements, needs to obtain the induced charge density according to the continuity equation of formation logging current in Formula (9).

2.2 Optimization Inversion of Wireless Communication

Wireless communication refers to the communication mode of information transmission without the use of wired cables or other physical connections. It uses electromagnetic waves to propagate in the air, allowing information transmission between two communication parties [22, 23]. The advantage of this communication mode is that it can avoid the restrictions brought by the physical connection, so that the communication can be carried out more freely without worrying about the line being damaged or affected by other factors. In the inversion process of sweep frequency dielectric logging, the developed forward inversion method is used to simulate the response law of tilt coil with sweep frequency dielectric logging tool in highly inclined wells and its application in geosteering [24, 25]. In order to effectively ensure the accuracy of inversion results of downhole geosteering, adaptive damping factors are added and inequality constraints are imposed to transform the forward problem of sweep frequency dielectric logging propagation resistivity into a nonlinear equation $F = F(x)$, $x = (x_1, \dots, x_N)^T$ downhole formation parameters representing the location to be measured, $F = (F_1, \dots, F_M)$ represents different function values, assuming f represent the function value of known measurement, then solve the unknown quantity x inversion problem of can be transformed into minimization f and $F(x)$ variance of is expressed by the following formula:

$$F' = \min \|f - F(x)\| \times H_{JJ} \tag{10}$$

In general, in order to make the whole iterative process stable, constraints need to be set when solving formula (20) $\|\delta x\| \leq \Delta$, Δ representing the maximum value of the given boundary, the inversion process of the entire tilt coil swept frequency dielectric logging model is transformed into solving the linear minimum equation problem with constraints:

$$D' = \min\{\|b - J\delta x\| : \|\delta x\| \leq \Delta\} \times F' \quad (11)$$

To solve formula (11), you need to $F(x)$ carry out forward calculation to obtain b On this basis, Jacobian matrix can be obtained through differentiation by forward modeling J , from which the satisfaction $\|\delta x\| \leq \Delta$ correction amount of. For Jacobian matrix J^T singular value decomposition is performed and expressed by the following formula:

$$J^T = U \times \Lambda V^T \times D' \quad (12)$$

Where, U and V On behalf of $M \times N$ and $N \times N$ matrix of order, Λ representative $M \times N$ diagonal matrix of order. In order to effectively reduce the multiplicity of the inversion problem, the change interval of the parameters of the swept frequency dielectric logging response numerical simulation model is taken as the prior information, which is expressed by the following inequality constraints:

$$\rho_{\min}^i \leq x_i \times J^T \leq \rho_{\max}^i, i = 1, 2, \dots, m \quad (13)$$

Where, x_i represents the parameters to be inverted, i represents the parameter number, ρ_{\min}^i and ρ_{\max}^i for and on behalf of i upper and lower limits of the parameters to be inverted. It should be noted that during the inversion process of sweep frequency dielectric logging, the change range of each inversion parameter can be more accurate according to other methods such as logging interpretation.

3 Numerical Simulation of Sweep Frequency Dielectric Logging Response

3.1 Scanning Frequency Dielectric Logging Directional Signal and Geological Directional Vector Angle

A variety of formation models are used to carry out inversion numerical simulation for swept frequency dielectric logging tool, and a new directional signal is defined for the structure of swept frequency dielectric logging tool receiving tilt coil, so that the structure of swept frequency dielectric logging receiving coil has the ability of downhole formation evaluation and geosteering azimuth detection. According to the above theoretical derivation. The dyadic Green's function of the magnetic dipole source can be obtained in the rectangular coordinate system of the downhole formation \tilde{G}^{HM} , \tilde{G}_{xz}^{HM} by z magnetic dipole in the direction of x For the magnetic field component generated in the direction, in order to effectively realize swept frequency dielectric azimuthal logging, it is necessary to extract the azimuthal signal, obtain new directional detection signal by using a new definition method, and subtract the phase difference and amplitude ratio signal on the receiving coil of the swept frequency dielectric logging

tool from the phase difference and amplitude ratio signal on different receiving coils of the lower transmitting coil:

$$\Delta\varphi' = \Delta\varphi_U - \Delta\varphi_D, A' = (A_U - A_D) \times (\rho_{\max}^i - \rho_{\min}^i) \quad (14)$$

where, $\Delta\varphi_U$ and A_U represents the phase difference and amplitude ratio obtained when the transmitting coil on the swept frequency dielectric logging tool works normally, $\Delta\varphi_D$ and A_D respectively represent the phase difference and amplitude ratio obtained when the lower transmitting ring of the swept frequency dielectric logging tool works, $\Delta\varphi'$ represents directional phase difference signal, A' represents the directional amplitude ratio signal. Generally, the resistivity of the downhole oil and gas reservoir is relatively high, and the reverse of the vector angle should be in the direction of the oil and gas reservoir. The direction of the swept frequency dielectric logging tool axis is defined as rectangular coordinates z axis direction, x axis is defined as the upward direction perpendicular to the ground, and the swept frequency dielectric logging tool xy plane is defined as the instrument face. When the transmitting antenna of the sweep frequency dielectric logging tool is axial and the receiving coil is transverse, the real and imaginary components of the geosteering vector on the surface of the sweep frequency dielectric logging tool can be expressed as follows:

$$s_b = (V_{xz}^r / \sqrt{(V_{xz}^r)^2 + (V_{yz}^r)^2}, V_{yz}^r / \sqrt{(V_{xz}^r)^2 + (V_{yz}^r)^2}, 0) \times \Delta\varphi' \quad (15)$$

$$x_b = (V_{xz}^i / \sqrt{(V_{xz}^i)^2 + (V_{yz}^i)^2}, V_{yz}^i / \sqrt{(V_{xz}^i)^2 + (V_{yz}^i)^2}, 0) \times \Delta\varphi' \quad (16)$$

Where, V_{xz}^r and V_{xz}^i represents the signal received on the swept frequency dielectric logging tool x real and imaginary parts of the component electromotive force, V_{yz}^r and V_{yz}^i respectively represent corresponding y real and imaginary parts of the component electromotive force, when the transmitting coil of the sweep frequency dielectric logging tool is inclined laterally and the receiving coil is axial, the downhole geological steering vector can be calculated using the following formula:

$$s'_b = (-V_{zx}^r / \sqrt{(V_{zx}^r)^2 + (V_{zy}^r)^2}, -V_{zy}^r / \sqrt{(V_{zx}^r)^2 + (V_{zy}^r)^2}, 0) \times s_b \quad (17)$$

$$x'_b = (-V_{zx}^i / \sqrt{(V_{zx}^i)^2 + (V_{zy}^i)^2}, -V_{zy}^i / \sqrt{(V_{zx}^i)^2 + (V_{zy}^i)^2}, 0) \times x_b \quad (18)$$

Where, V_{zx}^r and V_{zx}^i represents the transmitting coil of swept frequency dielectric logging tool x The real and imaginary parts of the electromotive force generated by the component magnetic field on the receiving coil, V_{zy}^r and V_{zy}^i respectively represent the corresponding transmitting coil y real and imaginary parts of the electromotive force generated by the component magnetic field of. According to the definition, the vector direction of the real part and imaginary part of the electromotive force both points to the more conductive area of the downhole formation, and the direction of its corresponding resultant vector indicates that the measured area of the swept frequency dielectric logging tool is more conductive in this direction, while the opposite direction of its resultant vector indicates the direction of higher formation resistivity.

3.2 Numerical Simulation and Anisotropy Measurement of Swept Frequency Dielectric Logging Geosteering Vector Angle

The space overlap algorithm is used to decompose the actual model, remove all the upper and lower surrounding rocks of the actual three-layer formation model, place the swept frequency dielectric logging tool in an infinite space, and after the above decomposition of the actual model, the relationship between the emf response tensor of the actual downhole three-layer formation model and the emf response tensor in the decomposed downhole three-layer formation model is $V = V_1 + V_2 - V_3$, V_1 , V_2 , V_3 represents the electromotive force tensor received in different models, V represents the total received electromotive force tensor of swept frequency dielectric logging tool, both of which are 3×3 . Assuming that it is necessary to tilt the transmitting coil and receiving coil to detect the anisotropy of the downhole formation, define T_6 and T_2 represent swept frequency dielectric logging transmitting coils, R_4 and R_3 respectively represent the receiving coil and measure separately T_6 and T_2 at launch R_4 and R_3 phase difference and amplitude ratio between, where R_4 and R_3 electromotive force on is only taken as a_0 phase difference and amplitude ratio signals of swept frequency dielectric logging are subtracted and used as the phase difference and amplitude ratio signals for detecting the anisotropy of the downhole formation, which are expressed by the following formula:

$$Att_a = \log \frac{[\text{Re}(a_0(T_6R_4))]^2 + [\text{Im}(a_0(T_6R_4))]^2}{[\text{Re}(a_0(T_6R_3))]^2 + [\text{Im}(a_0(T_6R_3))]^2} \quad (19)$$

$$PS_a = \tan^{-1} \frac{\text{Im}(a_0(T_6R_4))}{\text{Re}(a_0(T_6R_4))} \quad (20)$$

In the downhole homogeneous anisotropic medium, the above definition can be used to detect the anisotropic characteristics of the downhole formation. Taking the 500 kHz transmission frequency as an example, the phase difference and amplitude ratio under different horizontal and vertical resistivity contrast are calculated at 0° tilt angle, and shown in Fig. 1.

It can be seen from the figure that in a vertical well, when the downhole formation is thick, the horizontal and vertical resistivity of the downhole formation can be obtained by using the intersection diagram. When the horizontal resistivity of the transmitting coil of the swept frequency dielectric logging tool exceeds $15 \Omega \cdot \text{m}$, the sensitivity of the swept frequency dielectric logging tool to the formation anisotropy gradually decreases. When the well inclination angle gradually increases to 50° , the intersection diagram is shown in Fig. 2. It can be seen that. After the well inclination angle is gradually increased, the sensitivity of the swept frequency dielectric logging tool to the formation anisotropy is gradually increased. When the horizontal resistivity of the transmission coil of the swept frequency dielectric logging tool is $15 \Omega \cdot \text{m}$, the anisotropy of the downhole formation can be detected. Similarly, the intersection diagram under different inclination angles and arbitrary inclination frequencies can be drawn. In practice, according to the working mode of the sweep frequency dielectric logging tool and the inclination angle of the well, the intersection diagram is selected to obtain the anisotropy information of the downhole formation.

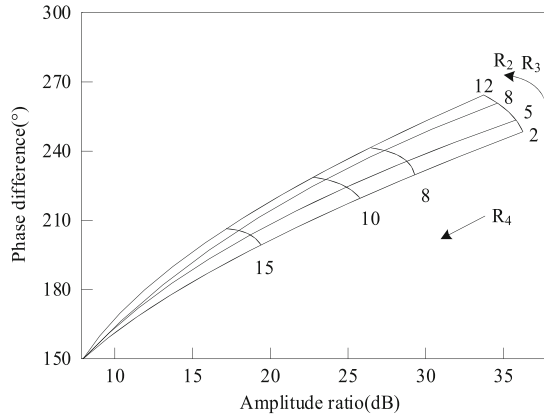


Fig. 1. Intersection Diagram of Phase Difference and Amplitude Ratio of Anisotropy at 500 kHz in Vertical Well

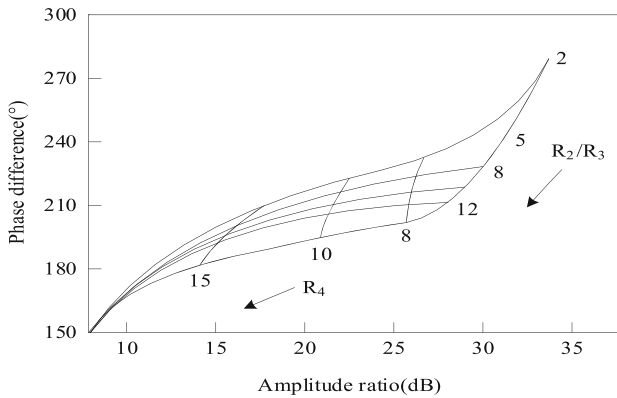


Fig. 2. Intersection Diagram of Phase Difference and Amplitude Ratio of Anisotropy at 400 kHz in 50° Relative Tilt Angle

4 Experimental Results and Analysis

Firstly, by comparing the numerical results of the swept frequency dielectric logging response, the validity of the numerical simulation model of the swept frequency dielectric logging response based on wireless communication proposed in this paper is verified. The response characteristics of the swept frequency dielectric logging are studied through the numerical simulation results on heterogeneous and anisotropic formations. During the numerical simulation of the swept frequency dielectric logging response, the long and short source distances of the coil system are 50 m, respectively. The short axis radius of the tilt coil is 30 cm, the transmission frequency is 500 kHz, and the borehole radius is 20 cm. Under the configuration of 2.4 GHz computer frequency and 4G memory, the sweep frequency dielectric logging response numerical simulation experiment is carried out. The experimental environment includes the electromagnetic field finite element analysis

software COMSOL Multiphysics and the swept frequency dielectric logging system. The experimental parameters include frequency range, transmission power, receiver distance, burial depth and dielectric constant. Specifically, according to the experimental requirements, the frequency range is 1 Hz to 1 GHz, the transmission power range is 10 dBm to 30 dBm, the receiver distance range is 1 m to 100 m, and the burial depth range is 1 m to 50 m. The rock dielectric constant is set to 2, 5, 10, 15, 20, 30, 40, 50, and 60 for testing. During the experiment, several simulations were carried out for each group of parameters, and the wireless communication response data under different parameters were collected and analyzed. The data is selected from iResearch data, and the website of the database is <http://www.iresearch.cn>. Through the collection and analysis of experimental data, the application of wireless communication technology in swept frequency dielectric logging is deeply studied and verified.

In order to more intuitively observe the inversion results, the inversion simulation of the following formations was carried out. The calculation conditions in Fig. 3 are: the borehole diameter is 40cm, the mud resistivity is 20 Ω·m, the target layer thickness is 20m, the horizontal resistivity of the downhole formation is 0°, and the resistivity of the formation surrounding rock is 90°. Figure 3 shows the influence of the downhole formation anisotropy coefficient on the sweep frequency dielectric logging response.

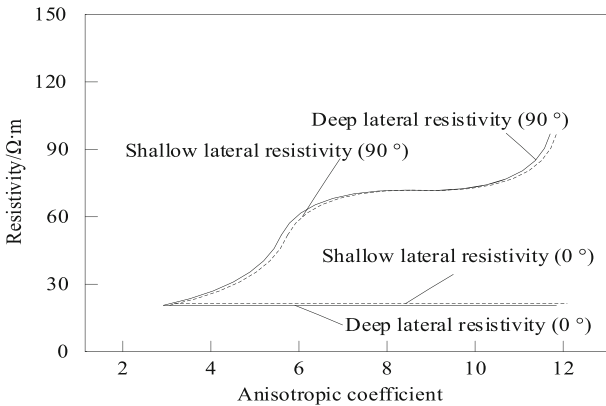
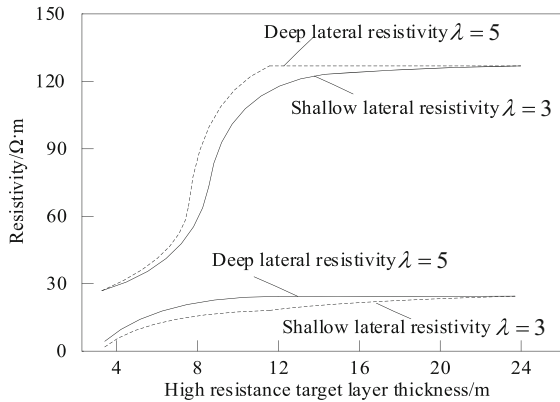


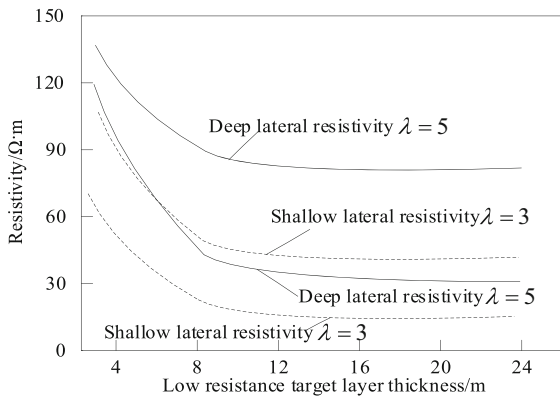
Fig. 3. Sweep frequency dielectric logging response changes with formation anisotropy coefficient at different well deflections

It can be seen from the analysis of Fig. 3 that the relationship between the swept frequency dielectric logging response and the variation of the layer anisotropy coefficient is quite different in the vertical well (0°) or horizontal well (90°) environment. In a vertical well, the current plane generated by the sweep frequency dielectric logging tool is parallel to the horizontal direction of the formation. The resistivity obtained by the sweep frequency dielectric logging tool basically comprehensively describes that the resistivity in the horizontal direction of the anisotropic formation changes little with the anisotropic formation coefficient, while in a horizontal well, the current plane generated by the sweep frequency dielectric logging tool is perpendicular to the horizontal downhole formation, Sweep frequency dielectric logging is obviously affected by vertical resistivity.

Figure 4 (a) The calculation model is the high resistivity of the target layer of the horizontal well. The resistivity in the horizontal direction is set as $50 \Omega \cdot m$. The surrounding rock of the underground formation is isotropic. The resistivity of the surrounding rock of the formation is $20 \Omega \cdot m$, the borehole diameter is $20cm$, and the mud resistivity is $2 \Omega \cdot m$. Figure 4 (b) The calculation model is the low resistivity of the target layer of the horizontal well. The corresponding horizontal resistivity is $5 \Omega \cdot m$, and the surrounding rock resistivity of the underground formation is $50 \Omega \cdot m$. As shown in Fig. 4, the sweep frequency dielectric logging response of the target layer with high resistance (a) and low resistance (b) of horizontal wells varies with the thickness of the layer under different downhole formation anisotropy conditions.



(a) Sweep frequency dielectric logging response of high resistivity target layer changes with layer thickness



(b) Change of sweep frequency dielectric logging response with formation thickness in low resistivity target formation

Fig. 4. Sweep Frequency Dielectric Logging Response of Target Layer of Horizontal Well Changing with Layer Thickness under Different Formation Anisotropy Conditions

As shown in Fig. 4, when the underground strata have different high resistivity and low resistivity, the influence of underground surrounding rock layer thickness on the response of swept-frequency dielectric logging is obviously different, but when the target is thin, the deep and shallow lateral resistivity of underground strata change obviously with the target layer thickness. When the underground strata thickness reaches a certain value, the corresponding resistivity reaches a certain value, and the changing trend of underground isotropic strata and anisotropic strata is similar. The above characteristics are due to the anisotropy of underground strata, which increases the vertical resistivity of swept-frequency dielectric logging, thus increasing the difference between the resistivity of underground target layer and the resistivity of surrounding rock.

In the actual sweep frequency dielectric logging environment, mud invasion causes the radial resistivity of permeable formation along the receiving coil to change. Due to the different detection depths of sweep frequency dielectric logging resistivity, the obtained resistivity has amplitude difference. Figure 5 calculates the target layer thickness of 8m, and the measured horizontal resistivity of the target layer is 50 Ω·m, the invasion radius is 0.9m, and the mud resistivity is 2 Ω·m.

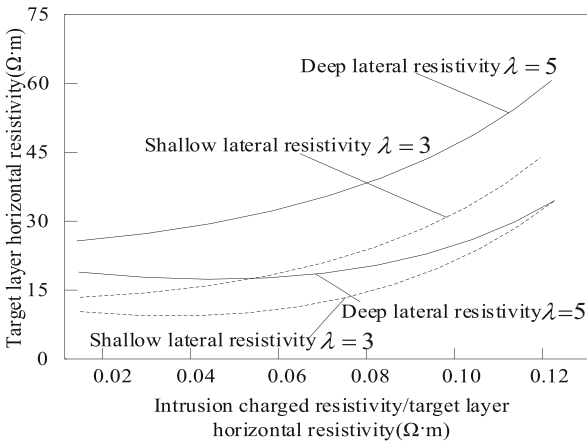


Fig. 5. Sweep frequency dielectric logging response changes with invasion resistivity under different formation anisotropy conditions

Analysis of Fig. 5 shows that mud invasion has obvious influence on the resistivity of swept-frequency dielectric logging. With the gradual increase of the resistivity of swept-frequency dielectric logging in invasion zone, the deep and shallow lateral resistivity of underground formation increases, while the amplitude difference gradually decreases, but the resistivity of anisotropic formation changes more sharply than that of isotropic formation, and the amplitude difference between deep and shallow lateral resistivity of swept-frequency dielectric logging increases gradually, which is more affected by mud invasion. Under the condition that the resistivity of swept-frequency dielectric logging in invasion zone is known,

5 Conclusion

In view of the interference of swept frequency dielectric logging signal caused by mud invasion in the current method, it can not meet the real-time requirements. Therefore, a numerical simulation model of swept frequency dielectric logging response based on wireless communication is proposed. According to the analysis of prior knowledge, the swept frequency dielectric logging response of anisotropic formation in horizontal wells is quite different from that in vertical wells. The results show that the swept frequency dielectric logging response of downhole anisotropic formation is mainly affected by the vertical resistivity of the formation. When the target formation has high resistivity, the anisotropic formation is greatly affected by the thickness of the surrounding rock under the well, and when the target formation has low resistivity, the downhole formation is greatly affected by the lateral formation. Compared with isotropic formation, mud invasion has more obvious and complex effects on the response of sweep frequency dielectric logging in downhole formation.

Acknowledgement. 2020 Teaching Research Project of Wuhan Institute of Design and Sciences: Case based “linear algebra” Hybrid Teaching Research and Practice (Project No.: 2020JY101).

References

1. Takahashi, A., Takyu, O., Fujiwara, H., et al.: Overloaded wireless MIMO switching for information exchanging through untrusted relay in secure wireless communication. *IEICE Trans. Commun.* **104**(10), 1249–1259 (2021)
2. Li, K., Li, Z., Xiong, Z., et al.: Thermal camouflaging MXene robotic skin with bio-inspired stimulus sensation and wireless communication. *Adv. Funct. Mater.* **32**(23), 1–10 (2022)
3. Yan, X., Pan, W., Zou, X., et al.: Optical frequency comb assisted denoising for multiple access and capacity enhancement of covert wireless communication. *Opt. Lett.* **47**(6), 1442–1445 (2022)
4. Zhang, F.F., Gao, R., Liu, J.: Acoustic wireless communication based on parameter modulation and complex Lorenz chaotic systems with complex parameters and parametric attractors. *Chin. Phys. B* **30**(8), 805–815 (2021)
5. Wang, A., Yang, L., Yi, X.J., et al.: Wireless communication applications of the variable inclination continuous transverse stub array for Ku-band applications. *IET Microw. Antennas Propag.* **15**(6), 644–652 (2021)
6. Okan, T.: High efficiency unslotted ultra-wideband microstrip antenna for sub-terahertz short range wireless communication systems. *Optik* **242**(1), 1–13 (2021)
7. Sharma, R.: RF analysis of double-gate junctionless tunnel FET for wireless communication systems: a non-quasi static approach. *J. Electron. Mater.* **50**(1), 1–17 (2021)
8. Huang, S., Safari, M.: SPAD-based optical wireless communication with signal pre-distortion and noise normalization. *IEEE Trans. Commun.* **70**(4), 2593–2605 (2022)
9. Liu, X., Chen, S., Song, L., et al.: Self-attention negative feedback network for real-time image super-resolution. *J. King Saud Univ. Comput. Inf. Sci.* **34**(8B), 6179–6186 (2022)
10. Han, C.W., Zhou, H., Liu, L., et al.: Power and rate control for wireless communication networks based on data. *Comput. Simul.* **39**(2), 375–379+511 (2022)
11. Liu, S., Li, Y., Fu, W.: Human-centered attention-aware networks for action recognition. *Int. J. Intell. Syst.* **37**(12), 10968–10987 (2022)

12. Liu, S., Gao, P., Li, Y., Weina, F., Ding, W.: Multi-modal fusion network with complementarity and importance for emotion recognition. *Inf. Sci.* **619**, 679–694 (2023)
13. Hu, S., Liu, W.N., Liu, Y.M., Liu, K.: Acoustic logging response law in shales based on petrophysical model. *Pet. Sci.* **19**(5), 2120–2130 (2022)
14. Liu, S., et al.: Human inertial thinking strategy: a novel fuzzy reasoning mechanism for IoT-assisted visual monitoring. *IEEE Internet Things J.* **10**(5), 3735–3748 (2023)
15. Li, Y., Chen, S., Liu, X., et al.: Study on the logging response characteristics and the quantitative identification method of solid bitumen at different thermal evolution stages. *Fuel* **316**(5), 1–16 (2022)
16. Liu, S., Xiyu, X., Zhang, Y., Muhammad, K., Weina, F.: A reliable sample selection strategy for weakly-supervised visual tracking. *IEEE Trans. Reliab.* **72**(1), 15–26 (2023)
17. Bisbing, S.M., Buma, B.J., Vander Naald, B., et al.: Single-tree salvage logging as a response to Alaska yellow-cedar climate-induced mortality maintains ecological integrity with limited economic returns. *For. Ecol. Manag.* **503**, 1–9 (2022)
18. Shen, J., Shu, D., Shen, Y., et al.: Response of casing hoop and geometry factor to transient electromagnetic logging in cased wells. *Geophys. Prospect.* **58**(4), 613–624 (2022)
19. Sun, J., Cai, J., Feng, P., et al.: Study on nuclear magnetic resonance logging T2 spectrum shape correction of sandstone reservoirs in oil-based mud wells. *Molecules* **26**(19), 1–10 (2021)
20. Sun, Z., Du, M., Xu, R., et al.: Wireless communication utilizing berry-phase carriers. *Laser Photonics Rev.* **16**(4), 1–9 (2022)
21. Alset, U., Mehta, H., Kulkarni, A.: Evaluation of antenna dependent wireless communication based on LoRa for clear line of sight (CLOS) and non-clear line of sight (NC-CLOS) applications. *J. Phys. Conf. Ser.* **1964**(3), 32–44 (2021)
22. Gummineni, M., Polipalli, T.R.: Implementation of reconfigurable emergency wireless communication system through SDR relay. *Mater. Today Proc.* **8**(3), 1–10 (2021)
23. Jassim, A.K.: Microstrip patch antenna with metamaterial using superstrate technique for wireless communication. *Bull. Electr. Eng. Inform.* **10**(4), 2055–2061 (2021)
24. Li, W., Lee, Y.H., Chen, Y.L., et al.: Proposed model for performance analysis of fourth-generation mobile wireless communication system. *Sens. Mater. Int. J. Sens. Technol.* **33**(4), 1375–1385 (2021)
25. Eid, M.M.A., Seliem, A.S., Rashed, A.N.Z., et al.: High modulated soliton power propagation interaction with optical fiber and optical wireless communication channels. *Indones. J. Electr. Eng. Comput. Sci.* **21**(3), 1575–1583 (2021)